AD-A172 049 SUPERSONIC MOLECULAR JET STUDIES OF THE PYRAZINE AND PYRIMIDINE DIMERS(U) COLORADO STATE UNIV FORT COLLINS DEPT OF CHEMISTRY J WANNA ET AL. 01 JUN 86 TR-20 1/1

UNCLASSIFIED N00014-79-C-0647 F/G 7/4 NL

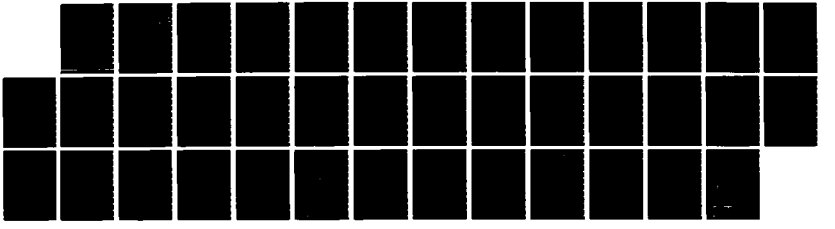

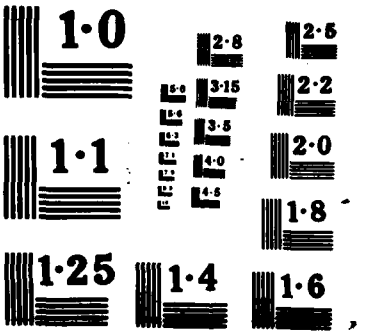
1·0
1·1
1·25
1·4
1·6
1·8
2·0
2·2
2·5
2·8
3·15
3·5
4·0
4·5

UNCLASSIFIED
SECURITY CLASSIFICATION OF THIS PAGE

AD-A172 049 (12)

REPORT DOCUMENTATION PAGE

1a. REPORT SECURITY CLASSIFICATION	1b. RESTRICTIVE MARKINGS
2a. SECURITY CLASSIFICATION AUTHORITY	3. DISTRIBUTION / AVAILABILITY OF REPORT Approved for public release; distribution unlimited.
2b. DECLASSIFICATION / DOWNGRADING SCHEDULE Unclassified	
4. PERFORMING ORGANIZATION REPORT NUMBER(S) N0014-79-C-0647	5. MONITORING ORGANIZATION REPORT NUMBER(S)
6a. NAME OF PERFORMING ORGANIZATION Colorado State University	6b. OFFICE SYMBOL (If applicable)
6c. ADDRESS (City, State, and ZIP Code) Department of Chemistry Fort Collins, Colorado 80523	7a. NAME OF MONITORING ORGANIZATION 7b. ADDRESS (City, State, and ZIP Code)
8a. NAME OF FUNDING / SPONSORING ORGANIZATION U.S. Army Research Office	8b. OFFICE SYMBOL (If applicable)
8c. ADDRESS (City, State, and ZIP Code) Post Office Box 12211 Research Triangle Park, NC 27709	9 PROCUREMENT INSTRUMENT IDENTIFICATION NUMBER N00014-79-C-0647
	10. SOURCE OF FUNDING NUMBERS PROGRAM ELEMENT NO. / PROJECT NO. / TASK NO. / WORK UNIT ACCESSION NO.

DTIC ELECTE SEP 19 1986 S E D

11. TITLE (Include Security Classification)
"Supersonic Molecular Jet Studies of the Pyrazine and Pyrimidine Dimers"

12. PERSONAL AUTHOR(S)
J. Wanna, J.A. Menapace and E.R. Bernstein

13a. TYPE OF REPORT	13b. TIME COVERED	14. DATE OF REPORT (Year, Month, Day)	15. PAGE COUNT
Technical	FROM _____ TO _____	June 1, 1986	30

16. SUPPLEMENTARY NOTATION The view, opinions, and/or findings contained in this report are those of the author(s) and should not be construed as an official Department of the Army position, policy, or decision, unless so designated by other documentation.

17. COSATI CODES			18. SUBJECT TERMS (Continue on reverse if necessary and identify by block number)
FIELD	GROUP	SUB-GROUP	

19. ABSTRACT (Continue on reverse if necessary and identify by block number)

Mass selected optical spectra for the first excited singlet $\pi\pi^*$ states of the pyrazine and pyrimidine dimers are presented. The species are created in a pulsed supersonic jet expansion. The spectra are analyzed based on ionization energy, vibronic structure and relative energy with respect to the isolated monomer (cluster spectroscopic shift). Calculations of binding energy and geometry for these dimers are carried out employing a Lennard-Jones (6-12-1) and hydrogen bonding (10-12-1) potential. In the case of pyrazine, calculations and experiments agree that both parallel planar hydrogen bonded and perpendicular dimers are present in the expansion. The calculations also predict a parallel stacked and 90° rotated pyrazine dimer which is not observed. This latter species most likely forms an excimer in the excited state with a short lifetime and a highly red shifted broad spectrum. In the case of pyrimidine, calculations yield four planar hydrogen bonded species and a parallel stacked and displaced species. The spectra for the pyrimidine dimer are consistent with these configurations, in agreement with the calculations. No perpendicular configuration

20. DISTRIBUTION / AVAILABILITY OF ABSTRACT	21. ABSTRACT SECURITY CLASSIFICATION
☒ UNCLASSIFIED/UNLIMITED ☐ SAME AS RPT ☐ DTIC USERS	UNCLASSIFIED
22a. NAME OF RESPONSIBLE INDIVIDUAL Elliot R. Bernstein	22b. TELEPHONE (Include Area Code) 303-491-6347 / 22c. OFFICE SYMBOL

DD FORM 1473, 84 MAR 83 APR edition may be used until exhausted. All other editions are obsolete.

SECURITY CLASSIFICATION OF THIS PAGE
UNCLASSIFIED

DTIC FILE COPY

Continued from Block 19 -

is calculated for the pyrimidine dimer and no spectroscopic features require postulating the existence of such a configuration. To explore further the agreement between calculated and experimental results for aromatic dimers, calculations are also presented for the tetrazine dimer. Three calculated geometries are obtained for the tetrazine dimer: a parallel stacked and 90° rotated species, a planar hydrogen bonded species and a perpendicular species. Experimental spectra and calculations are in basic agreement for all dimer studies and, in general, support one another.

OFFICE OF NAVAL RESEARCH

Contract N00014-79-C-0647

TECHNICAL REPORT #20

"SUPERSONIC MOLECULAR JET STUDIES OF THE PYRAZINE AND PYRIMIDINE DIMERS"

by

J. Wanna, J.A. Menapace and E.R. Bernstein

Prepared for Publication

in the

Journal of Chemical Physics

Department of Chemistry
Colorado State University
Fort Collins, Colorado 80523

May 1986

I. Introduction

Molecular dimers are of interest for a number of reasons. They can serve as model systems for condensed phase structure, dynamics, and nucleation and growth. Vibrational dynamics and reactions can be studied in clusters through the observation of vibrational dephasing or intramolecular vibrational redistribution (IVR) and vibrational predissociation (VP). Dimers also provide a model for higher order (i.e., secondary, tertiary, etc.) structure of more complex, flexible molecules. Finally, these small clusters can be treated as a new, weakly coupled state of matter appropriate in its own right for investigation and focused attention.

Small clusters or dimers are best studied by molecular jet techniques,[1-6] as the species are thereby isolated and free of extraneous perturbations. Of the molecular supersonic jet spectroscopy techniques available, the most useful is two-color time of flight mass spectroscopy[1] (2-color TOFMS) because many different clusters (e.g., dimers, trimers, dimers $(He)_n$, etc.) are simultaneously produced in the expansion process. 2-color TOFMS selects a cluster of particular mass, does not allow fragmentation of clusters to take place, thus maintaining mass integrity of the clusters, and yields a plot of cluster ion intensity in the chosen mass channel as a function of the cluster absorption spectrum.

Dimers of benzene, toluene and benzene-toluene have been studied in our laboratory using the 2-color TOFMS technique.[1] Coupled with the experimental findings, a potential energy calculation of the structure and binding energy of these dimers based on an exponential-six (exp-6) function has also been reported.[2] Spectroscopic data and potential energy calculations have been analyzed to arrive at a set of consistent geometries for these dimers. The benzene dimer is suggested to have a parallel displaced structure and the toluene and toluene-benzene dimers are suggested to have both parallel

displaced and perpendicular geometries. The benzene dimer characterization rests on isotopic substitution, absence of resolved splittings at the cluster 0_0^0, observation of only one feature respectively for $(C_6H_6)_2$, $(C_6D_6)_2$ and $C_6H_6C_6D_6$ at the cluster 0_0^0, and calculations employing the observed molecular quadrupole moment of C_6H_6 to set partial atomic charges and multipolar terms. In all instances, the experiments and calculations appear to arrive at self-consistent and independent conclusions which are in agreement with one another.

Molecular jet studies of other isolated dimers have also been reported. Rotationally resolved fluorescence excitation and dispersed emission spectra of tetrazine,[3] phenyltetrazine,[4] and dimethyltetrazine[5] dimers have been reported. Hydrogen bonded benzoic acid[6] and benzoic-acid-p-toluic acid[7] dimers have also been studied.

In this paper we report rotationally resolved 2-color TOFMS of pyrazine and pyrimidine isolated molecules at a resolution of 0.08 cm^{-1}. Unfortunately, this is insufficient resolution to obtain rotationally resolved 2-color TOFMS of the pyrazine and pyrimidine dimers. Computer simulations, based on a reasonable symmetric top algorithm, predict a resolution of at least 0.005 cm^{-1} (150 MHz) is needed to observe rotational structure for the dimers, assuming they are rigid.

In addition to the experimental spectroscopic methods used to study these dimers, potential energy calculations utilizing a Lennard-Jones (LJ; 6-12-1) potential are performed to yield minimum energy geometries and binding energies. This potential form is replaced with a LJ-hydrogen bonding (HB; 10-12-1) form for the appropriate set of atoms. The calculation and parameters employed are discussed and presented in an earlier publication.[8] These potentials, with literature parameter values, give the same results as the exp-6 with dipole-dipole, dipole-quadrupole, and quadrupole-quadrupole terms for

the benzene, toluene and benzene-toluene (and pyrazine and pyrimidine) dimers. The major advantage of the LJ form presently used in our studies is that more atomic parameters are available in the literature[9] and experimental multipole moments are not required for each system.

Dimer geometry is determined through analysis of experimental (*e.g.*, shifts, ionization energies, origin identification, vibronic analyses, etc.) and calculational results.

II. Experimental Procedures

A pulsed valve supersonic molecular jet system is used to generate the dimers. The pulsed valve is mounted in the mass spectroscopy chamber of a two chambered vacuum system. Since the duty cycle of the valve is roughly 10^{-3}, the 10 inch diffusion pump on the chamber and the 6 inch diffusion pump on the TOFMS flight tube adequately handle the gas load and maintain the chamber pressure below 2×10^{-6} torr. The system is described in previous publications.[1,8] The beam passes through a skimmer and then into the ionization region of a TOFMS. Two separately tunable lasers provide the photons for the $S_0 \rightarrow S_1$ transition and the $S_1 \rightarrow$ cluster ion transition.

Rotationally resolved 2-color TOFMS are obtained through pressure tuning of the grating box of the pump ($S_0 \rightarrow S_1$) dye laser oscillator cavity. The output of this laser is narrowed by an etalon placed between the dye cell and the grating in the oscillator cavity. The doubled output from this dye laser is 0.08 cm^{-1} in width. The laser can be scanned over roughly 20 cm^{-1} for a N_2 pressure variation of 10 to 1500 torr.

Pyrazine and pyrimidine are obtained from Aldrich Chemical Company and used without purification. The sample is placed in a trap behind the pulsed valve through which He flows at 120 psig.

The LJ potential energy function and calculational procedure have previously been described.[8] The additional constants needed for this work

are the (aromatic) N...H hydrogen bonding values: $B=8.244 \times 10^3$ kcal Å^{10}/mole and $A = 3.2897 \times 10^4$ kcal Å^{12}/mole. In order to check the LJ potential form, in particular for the pyrimidine dimer, LJ plus multipolar (i.e., drpole-dipole, dipole-quadrupole, and quadrupole-quadrupole) potential calculations are also performed.[2] The pyrimidine dipole and quadrupole moments[10] are taken to be -2.97×10^{-18} esu-cm and -1.91×10^{-26} esu cm^2, respectively.

Calculations are also reported which simulate the rotational structure of pyrazine and pyrimidine monomers and dimers. A symmetric top model is employed for this fit because it is simple, reasonably accurate, and in general is well suited to the purpose of roughly predicting the unresolved dimer structure. Both molecules are nearly symmetric tops ($\kappa \approx 0.9$). The form of the equations and methods employed are given by Herzberg.[11] The rotational temperature achieved in our system is ~2 K. The rotational constants used in the dimer rotational spectra calculations are found from the calculated LJ geometries. The molecular geometries can be found in ref. 12 for pyrazine and ref. 13 for pyrimidine.

III. Results

A. Pyrazine Dimer

The spectrum of the pyrazine dimer at the 0_0^0 transition is presented in figure 1 at two ionization energies, both of which are lower than the minimum ionization (second photon) energy of 44,000 cm^{-1} required to observe the 2-color TOFMS of the pyrazine monomer. Lowering the ionization energy from 43,182 cm^{-1} to 42,185 cm^{-1} causes three of the dimer related peaks to disappear: these features are found at -11.0, 12.0, and 26.2 cm^{-1} on the scale of figure 1. From the nature and appearance of these features, the +12 and +26 cm^{-1} peaks are quite likely vibrations built on the -11 cm^{-1} origin of a given configuration cluster. The intense features that

remain at the lower ionization energy are found at -26.3, -5.8, +34.1 and 50.7 cm^{-1}. From this variation of ionization energy one can determine that at least two configurations of the pyrazine dimer are present in the supersonic jet expansion. The pyrazine-d_4 dimer 0_o^o spectrum at two different ionization energies is presented in figure 2: the similarity between the pyrazine-h_4 and -d_4 dimer spectra is quite striking and reinforces our identification of origins and vdW vibronic features. The features that vanish at lower ionization energy are found at -11.5, 11.5, 25.5 and 64.1 cm^{-1} with respect to the pyrazine-d_4 0_o^o transition (31,030.4 cm^{-1}). These should be compared with the numbers in Table I. The features that remain with lower ionization energy are located at -26.9, -6.5, 31.0, and 45.9 cm^{-1}.

The spectra of the pyrazine dimer at other pyrazine vibronic origins are presented, along with the 0_o^o spectrum for comparison, in figure 3. The feature at roughly +61 cm^{-1} in this figure (+34.1 cm^{-1} in figure 1) is clearly an additional origin. The energy values and shifts for these features are presented in Table I. Since the pyrazine dimer is still observed at $10a_o^2$, its binding energy is greater than 800 cm^{-1}. No other features, appearing in the dimer mass channel, are found within -400 cm^{-1} of the pyrazine 0_o^o transition. The spectra of the pyrazine-d_4 dimer at these other vibronic monomer origins are again very similar to those of the pyrazine-h_4 dimer. We concluded from these spectra (not presented) that the third origin for the deuterated dimer lies at 31.0 cm^{-1} from the 0_o^o of the deuterated monomer.

Utilizing a Lennard-Jones potential function with a hydrogen bonding form, three configurations for the pyrazine dimer are calculated. Two of these configurations, a planar hydrogen bonded form and a perpendicular form, are displayed in figure 4. A parallel, stacked and 90° rotated structure is also found. The binding energies for the former two configurations are presented in the figure. In the planar geometry the ring centers are at 5.6 Å

from each other and the suggested C-H...N hydrogen bonds are 2.3 Å long. The pyrazine at the stem of the perpendicular configuration is situated in a symmetric position above the base pyrazine, with two of its hydrogens pointing to the base pyrazine nitrogens and equidistant from them. This perpendicular configuration has a 4.6 Å pyrazine center to center separation and apparent 2.6 Å H...N bond lengths.

B. Pyrimidine Dimer.

Three segments of the pyrimidine dimer 2-color TOFMS spectrum in the 0_0^0 region are displayed in figure 5 for two different ionization energies. Based only on the position and appearance of these segments we suggest that the features at -168 cm^{-1} and +296 cm^{-1} are each associated with different geometries. The grouping of features in the +170 cm^{-1} region must be associated with more than one dimer configuration, as these eight sharp, relatively intense features are clearly not vdW vibronic progressions built on a single 0_0^0 origin. The minimum ionization energy for the pyrimidine monomer is near 44,090 cm^{-1} above the $^1B_1$ ($n\pi^*$) excited state at 31,073 cm^{-1}. As can be seen from figure 5, features in two of the three regions displayed disappear as the ionization energy is lowered from 44,363 cm^{-1} to 42,320 cm^{-1}.

Calculations using a LJ-HB potential function yield four planar configurations, a parallel stacked head-to-tail displaced configuration, and a parallel stacked undisplaced configuration with the two pyrimidine molecules rotated 90° with respect to each other. The latter configuration most likely does not contribute to the observed dimer spectrum since it will probably form an excimer. No perpendicular geometry is calculated even with the LJ-HB potential augmented with multipolar terms. Figures 6 and 7 give those calculated geometries for the pyrimidine dimer which can produce the observed spectral features. The parallel displaced geometry shown in figure 6 is head-to-tail displaced by 0.6 Å along the CH-CH line from the molecular center; the

interplane separation is 3.3 Å. The calculated binding energy for this dimer is 1478 cm^{-1}.

The planar configurations are displayed in figure 7. Configuration I has a center to center distance of 5.5 Å, two N---H hydrogen bonds (2.3 Å separation), and a calculated binding energy of 709 cm^{-1}. Configurations II, III, and IV also display some hydrogen bonding but to a lesser extent than that displayed in configuration I. In these latter three cases, the less "acidic" hydrogens, not between the two N atoms, are involved in the "hydrogen bonds": the pyrimidine molecule center to center distance is ~6.0 Å and the calculated binding energies range from 400 cm^{-1} to 430 cm^{-1}, substantially less than the binding energy for configuration I. Configuration II has two N--H hydrogen bonds each of 2.9 Å. Configurations III and IV have a nitrogen atom of one pyrimidine equidistant from two hydrogens of the other pyrimidine with an apparent hydrogen bond distance of 2.9 Å. Planar configurations in which two nitrogens are facing each other are not stable.

C. Rotational Structure.

Rotationally resolved 2-color TOFMS data can be obtained for the pyrazine and pyrimidine monomers using the resolution presently available in our laboratory ($\Delta\nu \sim 0.08$ cm^{-1}). The spectra are presented in figure 8. These well resolved spectra evidence a central Q-branch with well developed R and P branches to the high and low energy sides, respectively. The calculated rotational structures for these transitions are presented in figure 9. In order to make the fit look reasonable, a 0.1 cm^{-1} gaussian line width was incorporated in the calculated spectrum.

Considering that a symmetric top equation is used for the fit, the agreement between the calculated and experimental results is excellent. The purpose of this exercise is to observe and calculate the rotational spectrum of a dimer. One can see from figure 10 (top) that the rotational structure of

the pyrazine dimer is not evident at this laser linewidth. Similar conclusions arise from the spectra of the benzene dimer (see figure 11). Computer simulations of the pyrazine dimer spectrum (based on the symmetric top calculations), show that a ca. 0.005 cm^{-1} laser linewidth is required to resolve rotational transitions for the aromatic dimers (fig. 10 bottom). An attempt to fit the rotational contours to parallel or perpendicular transitions of parallel or perpendicular dimers demonstrates that no convincing conclusions concerning dimer geometry can be reached in this manner. In fact, the spectra of the parallel and perpendicular pyrazine dimer origins do not appear different at this resolution. The calculated contours are found using rotational constants of $A'' = 0.0611$, $B'' = 0.0157$ and $C'' = 0.0141$ cm^{-1} for the perpendicular dimer and $A'' = 0.0381$ $B'' = 0.0153$ and $C'' = 0.0112$ cm^{-1} for the parallel planar dimer.

IV. Discussion

A. Pyrazine Dimer.

In the following paragraphs, only the pyrazine-h_4 dimer results will be discussed in detail. The similarity between the pyrazine-h_4 and -d_4 dimer results obviates the need for discussion of these data separately.

One of the most important experimental observations concerning the pyrazine dimer is the change in the spectrum as a function of ionization laser or second photon energy. Lowering the ionization laser energy by 1000 cm^{-1} to 42,185 cm^{-1} causes three features to disappear: two of these are assigned as vibrations built on a single origin (see Table I and figure 1). Further reduction of the ionization energy to 41,721 cm^{-1} results in no observed TOFMS spectrum for the pyrazine dimer. At least two different geometries of the pyrazine dimer are therefore present in the beam. The dimer with the higher ionization energy is probably a symmetrical dimer with two symmetry equivalent molecules because only one origin is associated with the high ionization energy spectrum.

Different geometries will possess different ionization energies depending on the involvement of the π-clouds in the overall dimer interaction. For example, a planar hydrogen bonded dimer would probably have a poor ion "solvation" or stabilization and might therefore have a higher ionization energy. This geometry would in addition have only one spectroscopic origin. A perpendicular geometry dimer would, on the other hand, probably evidence two features and a lower ionization energy due to the π-cloud involvement of the "horizontal" pyrazine in the stabilization of the ion.

The calculations give three general geometries for the pyrazine dimer: a parallel planar, a perpendicular, and a parallel stacked and 90^{o} rotated geometry. The latter geometry is not discussed in this work because it likely is not important for any of the spectroscopic observations presented earlier. The remaining two configurations give rise to three separate spectra: one for the parallel planar geometry (I) and two for the perpendicular geometry (base IIa and ster IIb).

Table I gives the assignment of the dimer spectra. The planar geometry (I) is assigned to the origin at -11 cm^{-1} (figure 1) since this single origin feature is associated with the higher ionization energy. The other two origins at -26.5 cm^{-1} and +34.1 cm^{-1} (figure 1) with respect to the pyrazine monomer origin are assigned to the perpendicular dimer because they both show the same low ionization energy. The base (IIa) is associated with the red shifted origin and the stem (IIb) is associated with the blue shifted origin. This latter correlation between spectra and calculated structures is based on the argument presented in previous publications[1,2] relating solvent cluster shifts and π-cloud involvement in the solute-solvent interaction: the larger the red shift, the more direct is the interaction between the -system and the solvent. Thus the base molecule should be expected to have a larger red shift than the stem molecule.

The pyrazine $6a^1$ (in-plane C-C stretch) and $10a^1$ (out-of-plane C-C bend) vibrational modes show strong interaction with the van der Waals modes (figure 3).

B. Pyrimidine Dimer

The ionization energy for the pyrimidine dimer system is again an important piece of information used to help determine the number of different configurations responsible for the observed spectra and, perhaps, their geometry. Lowering the ionization by 2,043 cm^{-1} to 42,320 cm^{-1} causes the feature at -168 cm^{-1} to disappear, the features at ca. +175 cm^{-1} nearly to disappear, and the feature at +296 cm^{-1} to reduce in intensity. In addition, dimer spectral shifts can also be employed to associate calculated geometries with spectroscopic features: red shifted origins can be assigned to parallel stacked geometries, and blue shifted origins to planar hydrogen bonded forms. Perpendicular geometries can be responsible for both red and blue shifts depending on which molecule of the dimer is involved.[1]

LJ-HB potential calculations suggest one parallel stacked head-to-tail displaced, one parallel stacked rotated, and four parallel planar configurations for the pyrimidine dimer. No perpendicular geometry can be calculated using LJ-HB or a multipolar form.[1,2] All calculations give nearly identical geometries and binding energies for the parallel planar and stacked configurations.

The feature at -168 cm^{-1} is suggested to be due to the parallel stacked and displaced head-to-tail geometry. One would expect this structure to have only one spectroscopically observed 0_0^0 transition and a substantial red shift. The remaining features in the spectra, due to their significant blue shifts, must be attributed to planar hydrogen bonded dimers. The feature at +296 cm^{-1} is suggested to be due to configuration I shown in figure 7. This configuration of the pyrimidine dimer forms two hydrogen bonds both of

which involve the hydrogen atoms between the two ring nitrogen atoms on each pyrimidine: these hydrogens are the most electropositive (acidic) hydrogens on the ring. This configuration also has the monomers closest to each other (5.5 Å compared to 6.0 Å in the others). These factors suggest that configuration I gives rise to the most blue shifted feature in the spectra. The remaining three configurations II, III, and IV must generate the features in the +175 cm^{-1} region. Configuration II is a symmetrical dimer and will account for one feature while configurations III and IV each will account for two features since the pyrimidines in these last two configurations are not symmetry equivalent. Assigning these features to configurations II, III, and IV is a difficult task without further information: five of the eight major features in this region can, however, be associated with origins of configurations II, III, and IV.

The parallel planar hydrogen bonded configuration I is assigned to the large blue shift, low ionization energy feature and the parallel stacked displaced geometry is assigned to the large red shifted, high ionization energy feature. On the other hand, the parallel planar pyrazine dimer is assigned to the feature with the higher ionization energy (and also a small red shift). Clearly the two dimers have a very different electronic structure and the component monomers must interact in a different manner. A possible explanation for these apparent differences is that the N-C-N moiety of the pyrimidine system becomes the positive end of the molecular ion which is in turn well solvated in the parallel planar dimer thus lowering the ionization energy, and that the loss of electron density in the N-C-N region in the $n\pi^*$ excited state reduces the hydrogen bond energy thus increasing the energy of the excited S_1 state and causing a dimer blue shift. Similar arguments can be rendered to

rationalize a negligible shift for the pyrazine system. We caution, however, that all such qualitative reasoning is subject to verification by more rigorous quantum mechanical calculations.

To ensure that our LJ-HB potential can produce other perpendicular dimer configurations, we have calculated the geometries expected for the tetrazine system. The tetrazine dimer has been studied by Levy and co-workers,[3] who have reported two geometries: a parallel planar configuration and a perpendicular configuration. These experiments involve rotationally resolved fluorescence excitation spectra. Our calculations generate three geometries for this dimer: a parallel planar configuration, a parallel, stacked and 90° rotated configuration, and a perpendicular configuration, as shown in figure 12. The calculated perpendicular configuration has one hydrogen of the stem tetrazine pointing towards an N-N bond of the base tetrazine. In this configuration the plane of the stem tetrazine bisects the two N-N bonds of the base tetrazine. Levy's published perpendicular configuration[3a] has one hydrogen of the two C-H bonds of the stem tetrazine pointing toward one C-H bond of the base tetrazine and the plane of the stem tetrazine passing through the two C-H bonds of the base tetrazine. Rotational constants reported by Levy and obtained from a rotational analysis of the perpendicular configuration for parallel polarization are A" = 0.07287 cm^{-1}, B" = 0.01722 cm^{-1}, and C" = 0.01649 cm^{-1}. Rotational constants obtained from our calculated perpendicular configuration are A" = 0.06458 cm^{-1}, B" = 0.01644 cm^{-1}, and C" = 0.018466. These two sets of rotational constants render reasonably similar spectra, as can be seen in fig. 13.

V. Conclusion

The analysis of the structure and properties of the pyrazine and pyrimidine dimers is based on an interpretation of ionization energy dependence, van der Waals vibronic structure, dimer spectral shifts, and potential energy calculations with LJ-HB and multipolar forms.

Variation of the ionizing laser energy allows different configuration dimers of a particular species to be identified. The pyrazine (h_4 and d_4) dimer has two identified geometries based on ionization energy dependence and vibronic analysis. Given the dimer spectral shifts and calculations, these have been associated with a planar parallel hydrogen bonded configuration and a perpendicular configuration. A third geometry, planar stacked and rotated 90^o, is calculated but not observed probably due to excimer formation.

The pyrimidine dimers absorb in three spectral regions. The lowest energy feature is thought to be the calculated head-to-tail parallel stacked displaced geometry, the highest energy feature is assigned as a parallel planar strongly hydrogen bonded form in which the most electropositive H-atoms are involved in the hydrogen bonding. The features at +175 cm^{-1} are attributed to different planar configurations which are only weakly hydrogen bonded through the less acidic hydrogens on the rings.

Dimer spectral shifts are expected to follow the rules determined previously for solute-solvent clusters: the major red shift mechanism is π-system coordination or overlap between the two molecules and the major blue shift mechanism is hydrogen bonding. Ionization energies can be rationalized in accordance with the general notions of ion solvation by either the π-system in the case of pyrazine or the N-C-N hydrogen bonding region in the case of pyrimidine.

Calculations are also presented for the tetrazine dimers to compare parallel planar and perpendicular spectroscopically assigned geometries and our calculations. Calculations predict, and experiments suggest, perpendicular geometries for toluene, benzene-toluene, pyrazine, and tetrazine but not for benzene. Moreover, calculations predict, and experiments are consistent with, the absence of perpendicular geometries for the pyrimidine dimer. Perhaps one of the most remarkable results of this study is the rather large number of

different, roughly equal binding energy configurations found for the N-heterocyclic aromatic dimers in general.

REFERENCES

1. K.S. Law, M. Schauer, and E.R. Bernstein, J. Chem. Phys. 81, 4871 (1984).
2. M. Schauer and E.R. Bernstein, J. Chem. Phys. 82, 3722 (1985).
3. a. C.A. Haynam, D.V. Brumbaugh, and D.H. Levy, J. Chem. Phys. 79, 1581 (1983);
   b. L. Young, C.A. Haynam, and D.H. Levy, J. Chem. Phys. 79, 1592 (1983).
4. Y.D. Park and D.H. Levy, J. Chem. Phys. 81, 5527 (1984).
5. D.V. Brumbaugh, C.A. Haynam, and D.H. Levy, J. Chem. Phys. 73, 5380 (1980).
6. D.E. Poeltl and J.K. McVey, J. Chem. Phys. 78, 4349 (1983).
7. Y. Tomioka, H. Abe, N. Mikami, and M. Ito, J. Phys. Chem. 88, 5186 (1984).
8. J. Wanna and E.R. Bernstein, J. Chem. Phys. 84, 927 (1986).
9. a. F.A. Momany, L.M. Carruthers, R.F. McGuire, and H.A. Scheraga, J. Phys. Chem. 78, 1595 (1974);
   b. G. Nemethy, M.S. Pottle, and H.A. Scheraga, J. Phys. Chem. 87, 1883 (1983).
10. F. Mulder, G. Van Dijk, and C. Huiszoon, Mol. Phys. 38, 577 (1979).
11. G. Herzberg, Molecular Spectra and Molecular Structure II. Infrared and Raman Spectra of Polyatomic Molecules (Van Nostrand Reinhold Co., 1945) Chapters I and IV.
12. P.J. Wheatley, Acta Crys. 10, 182 (1957).
13. P.J. Wheatley, Acta Crys. 13, 80 (1960).

Table I
Pyrazine Dimer

Energy (vac. cm^{-1})	Energy Relative to Corresponding Pyrazine Feature (cm^{-1})	Energy Relative to Corresponding Pyrazine Dimer Feature (cm^{-1})	Assignments[a]
30849.5	-26.5	0	II base 0_o^o
30865.0	-11.0	0	I 0_o^o
30870.2	- 5.8	20.7	
30879.1	3.1	29.6	
30888.0	12.0	23.0	
30891.4	15.4	41.9	
30898.7	22.7	49.2	
30902.3	26.3	37.3	
30910.1	34.1	0	II stem 0_o^o
30914.0	38.0	3.9	
30918.2	42.2	8.1	
30926.7	50.7	16.6	
31228.5	-30.5	0	II base $10a_o^1$
31238.5	-20.5	0	I $10a_o^1$
31245.4	-13.6		
31254.8	- 4.2		
31289.4	30.4	0	II stem $10a_o^1$
31297.6	38.6		
31314.4	55.4		

Table I
Pyrazine Dimer
(Continued)

Energy (vac. cm^{-1})	Energy Relative to Corresponding Pyrazine Feature (cm^{-1})	Energy Relative to Corresponding Pyrazine Dimer Feature (cm^{-1})	Assignments[a]
31433.3	-26.4	0	II base $6a_o^1$
31445.1	-14.6	0	I $6a_o^1$
31456.8	- 2.9		
31467.8	8.1		
31481.7	22.0		
31488.9	29.2		
31493.2	33.5	0	II stem $6a_o^1$
31507.9	48.2		
31565.7	106.0		
31677.9	-21.1	0	II base $10a_o^2$
31686.1	-12.9	0	I $10a_o^2$

[a] See figure 4.

FIGURE CAPTIONS

Figure 1 Two-color TOFMS of the pyrazine dimer in the region of the pyrazine origin at two different ionization energies, top trace at an ionization energy of 43,182 cm^{-1} and the lower trace at an ionization energy of 42,185 cm^{-1}. The pyrazine origin at 30,876 cm^{-1} lies at 0 cm^{-1} on the scale of the figure.

Figure 2 Two-color TOFMS of the pyrazine-d_4 dimer in the region of the pyrazine-d_4 origin. Two different ionization energies are presented. The pyrazine-d_4 monomer origin lies at 0 cm^{-1} on the scale of the figure. Compare to figure 1 for the pyrazine-h_4 dimer.

Figure 3 Two-color TOFMS of the pyrazine dimer in the 0_o^o, $10a_o^1$ and $6a_o^1$ regions. These spectra are taken at high (ca. 43,200 cm^{-1}) ionization energy.

Figure 4 Minimum energy configurations and binding energies for pyrazine dimer as obtained with a LJ plus HB potential calculation.

Figure 5 Three segments of the 2-color TOFMS spectra of the pyrimidine dimer at two ionization energies, top trace at an ionization energy of 44,363 cm^{-1} and the lower trace at an ionization energy of 42,320 cm^{-1}. The energy scale is relative to the pyrimidine monomer 0_o^o.

Figure 6 Minimum energy configuration and binding energy for the stacked pyrimidine dimer as obtained with a LJ plus HB potential calculation.

Figure 7 Minimum energy configurations and binding energies for the planar pyrimidine dimers as obtained with a LJ plus HB potential calculation.

Figure 8 Two-color TOFMS rotational spectra of the origins of pyrazine (top) and pyrimidine (bottom) monomers.

Figure 9 Simulated rotational spectra of the pyrazine and pyrimidine origins.

Figure 10 Two-color TOFMS rotational spectrum of the pyrazine dimer origin (top) and computer simulated rotational spectrum of the pyrazine dimer origin (bottom). The origin is at 30,849.5 cm^{-1} (-26.5 cm^{-1} origin in figure 1). The FWHM is roughly 2 cm^{-1}. The 30,865.0 cm^{-1} origin looks nearly identical to this one at the experimental resolution.

Figure 11 Two-color TOFMS of the benzene dimer 0_0^0 transition at 0.08 cm^{-1} resolution. Most of the "features" in this trace are noise and are not reproducible.

Figure 12 Minimum energy configurations and binding energies for the tetrazine dimer as obtained with a LJ plus HB potential calculation.

Figure 13 Calculated rotational contours of the parallel polarized transition of the perpendicular tetrazine dimer centered at 18272.0 cm^{-1} (0 cm^{-1} in the figure). The upper trace is calculated using the rotational constants obtained from the perpendicular configuration reported in ref. 3a. The lower trace is calculated using the rotational constants obtained from the perpendicular configuration reported in this work. A symmetric top model is assumed for both calculations and the intensities used are those of ref. 3a. The rotational constants employed are given in the text; in the symmetric top approximation $\bar{B}'' = \frac{B'' + C''}{2}$.

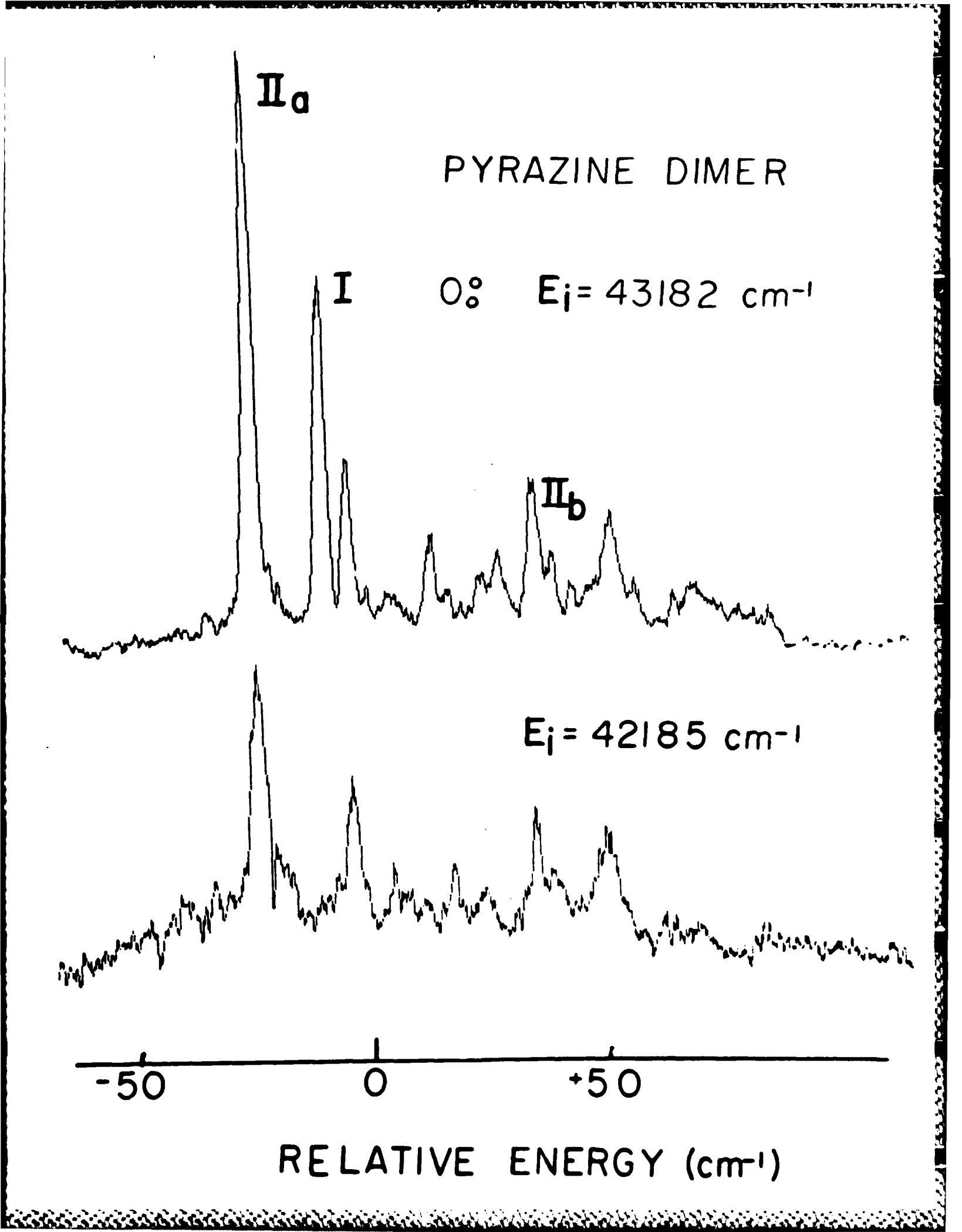
IIa
PYRAZINE DIMER
I
0°
Ei = 43182 cm-1
IIb
Ei = 42185 cm-1
-50
0
+50
RELATIVE ENERGY (cm-1)

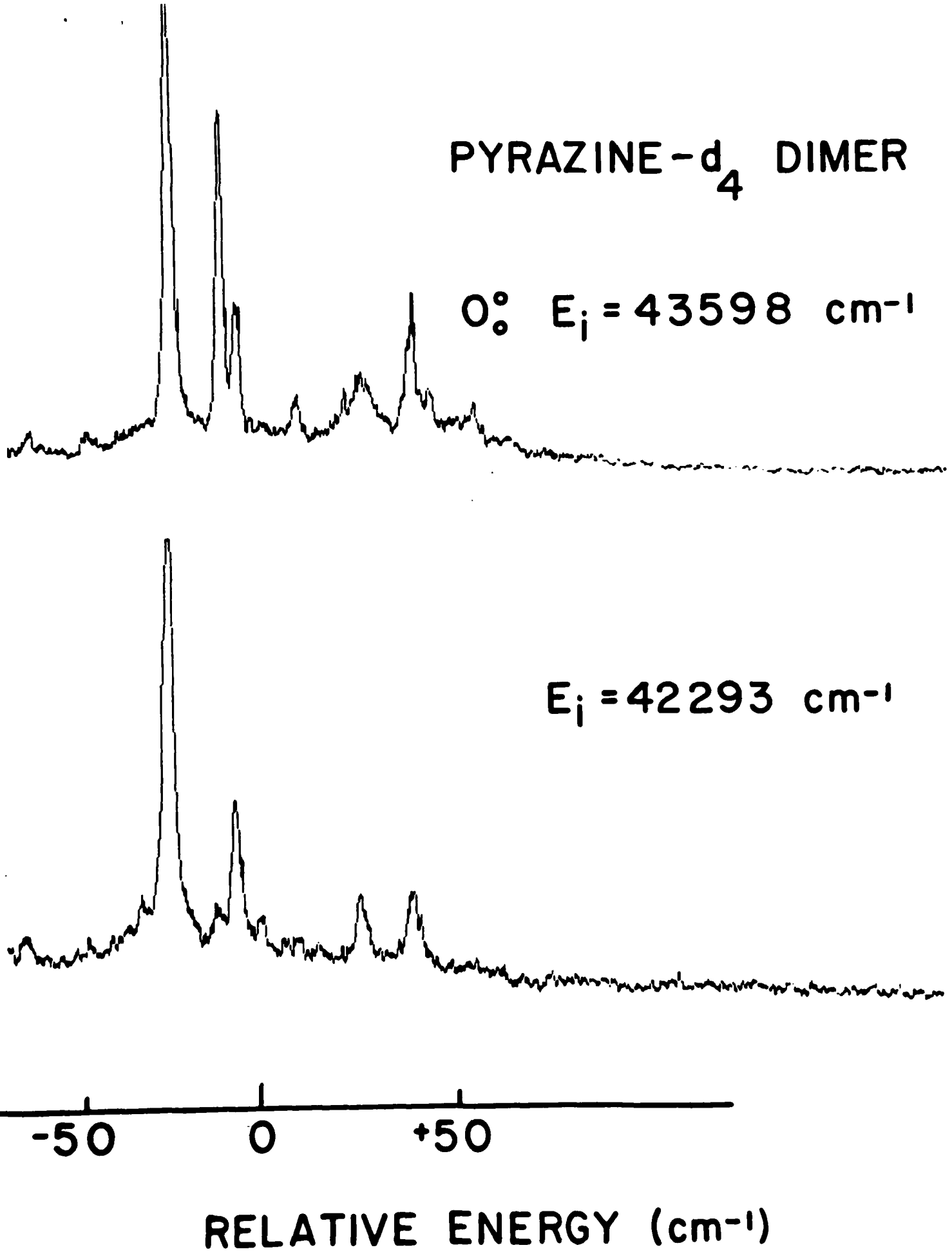
PYRAZINE-d_4 DIMER
0° E_i = 43598 cm^{-1}
E_i = 42293 cm^{-1}
-50
0
+50
RELATIVE ENERGY (cm^{-1})

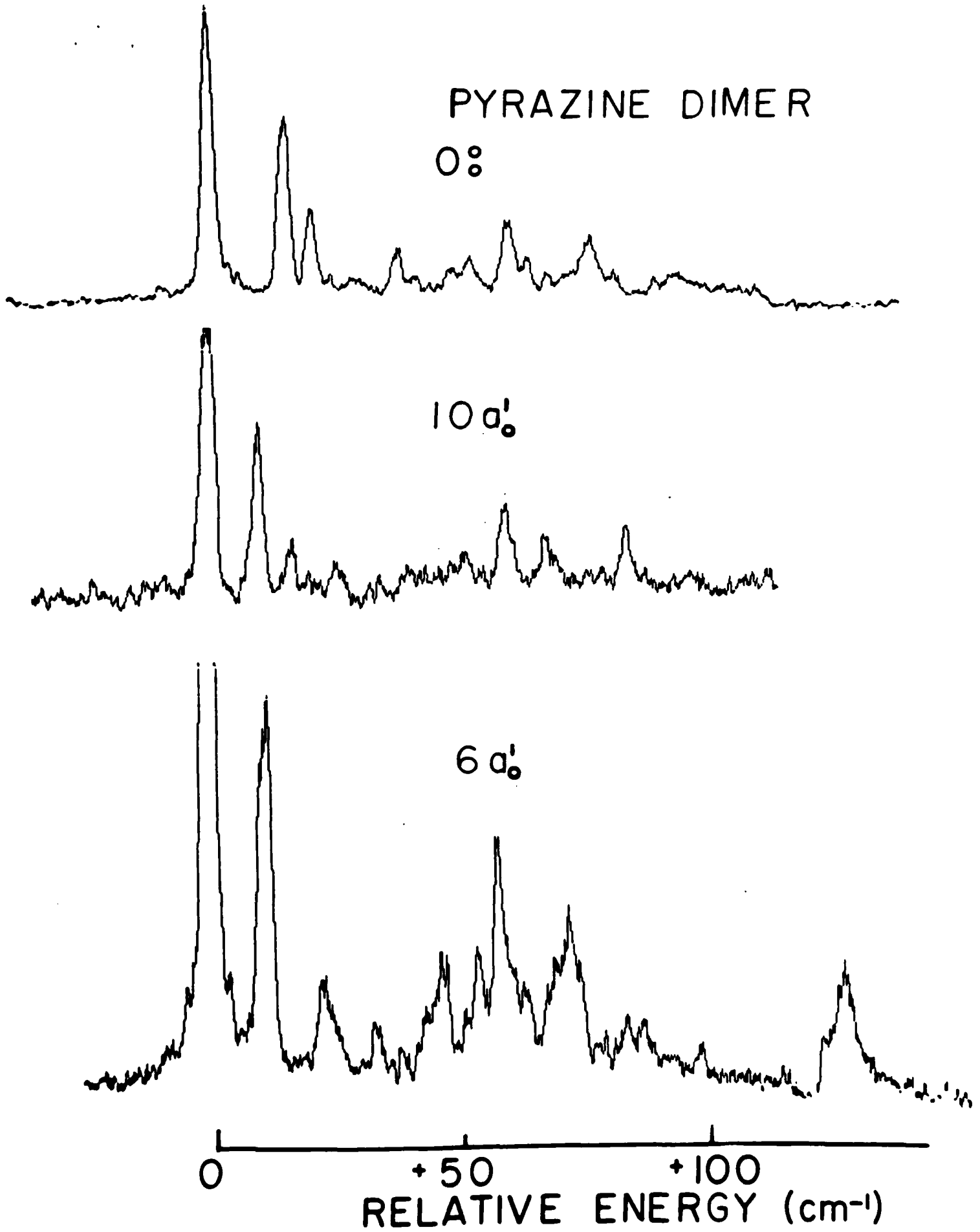
PYRAZINE DIMER
0₀
10 a'₀
6 a'₀
0
+50
+100
RELATIVE ENERGY (cm⁻¹)

PYRAZINE DIMER

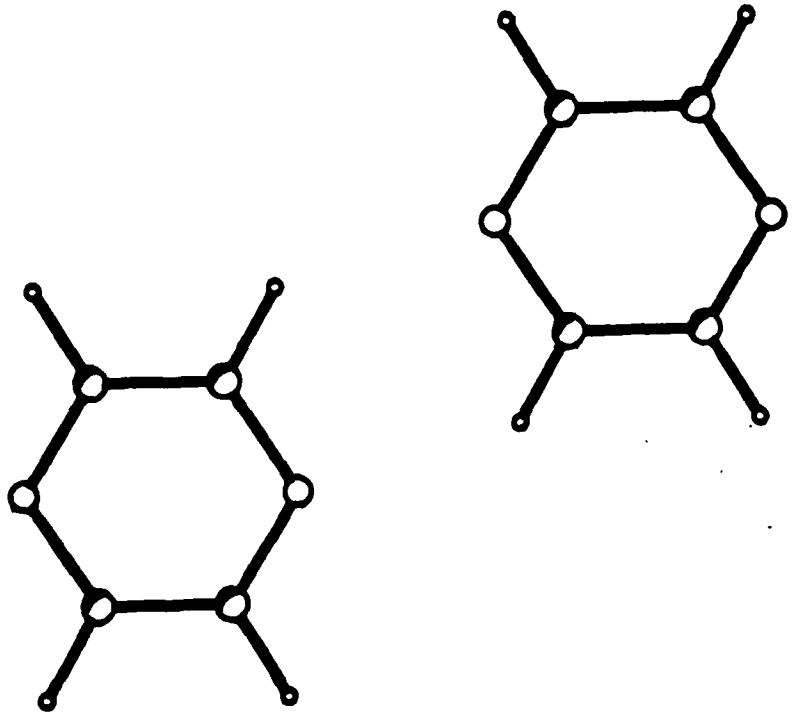

I -716 cm^{-1}

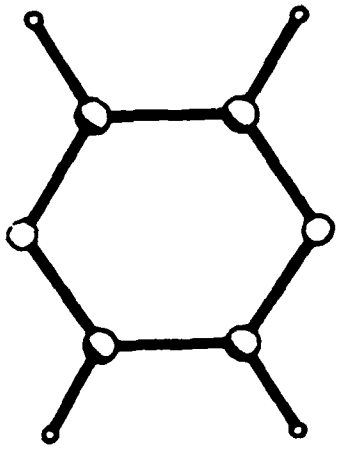

II -854 cm^{-1}

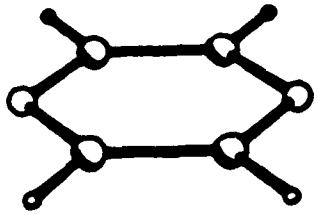

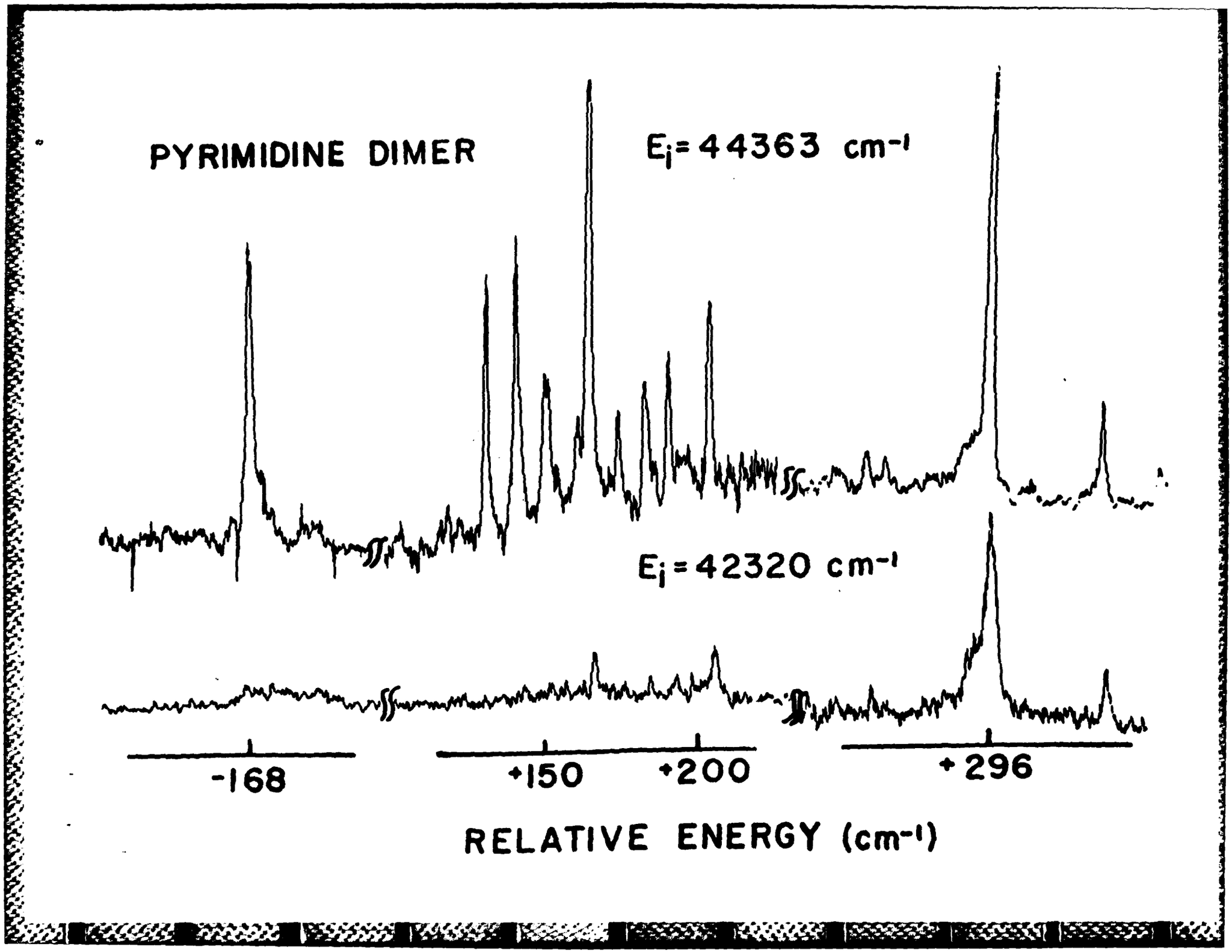
PYRIMIDINE DIMER
$E_i = 44363\ cm^{-1}$
$E_i = 42320\ cm^{-1}$
-168
+150
+200
+296
RELATIVE ENERGY (cm^{-1})

PYRIMIDINE DIMER

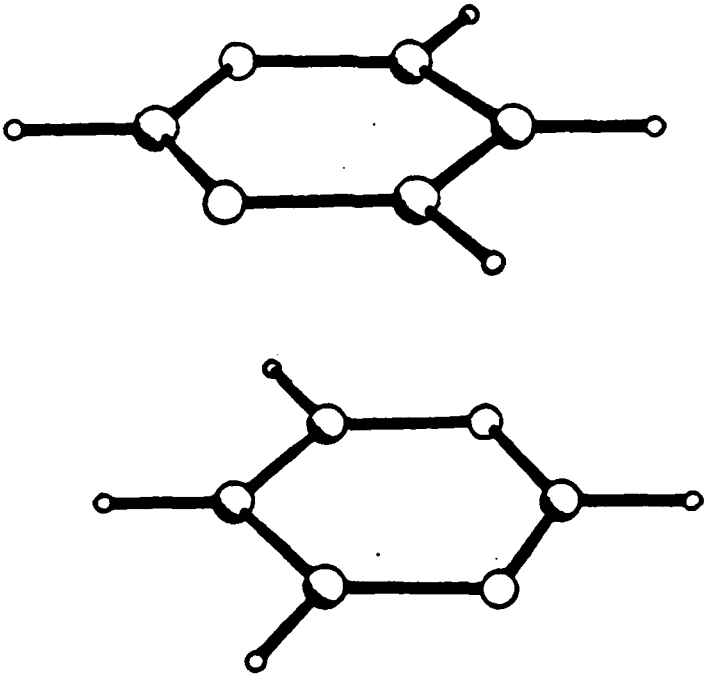

-1478 cm^{-1}

PYRIMIDINE DIMER

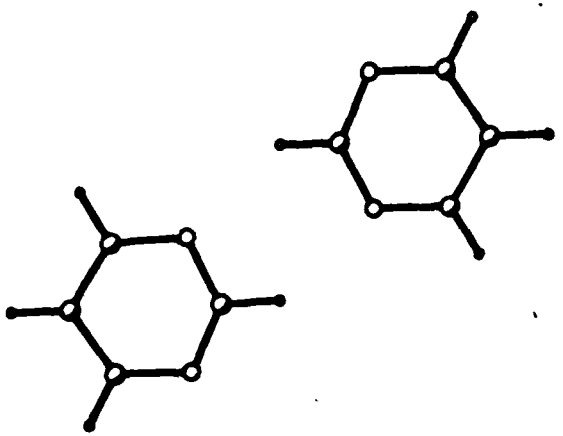

I

-709 cm^{-1}

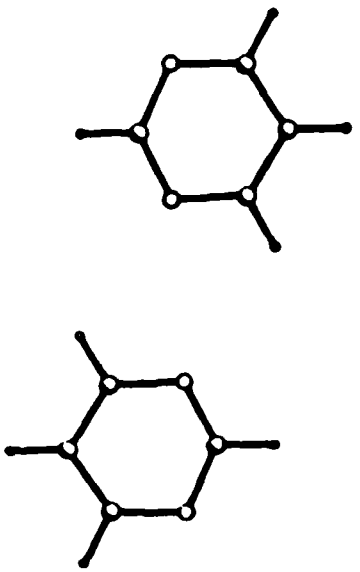

II

-402 cm^{-1}

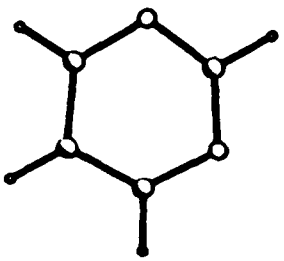

III

-422 cm^{-1}

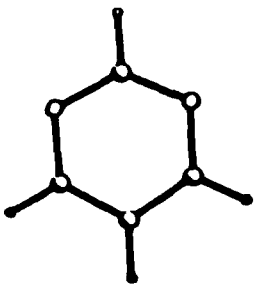

IV

-429 cm^{-1}

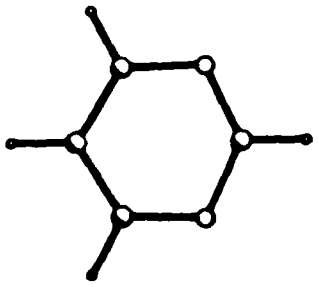

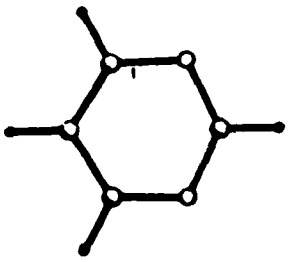

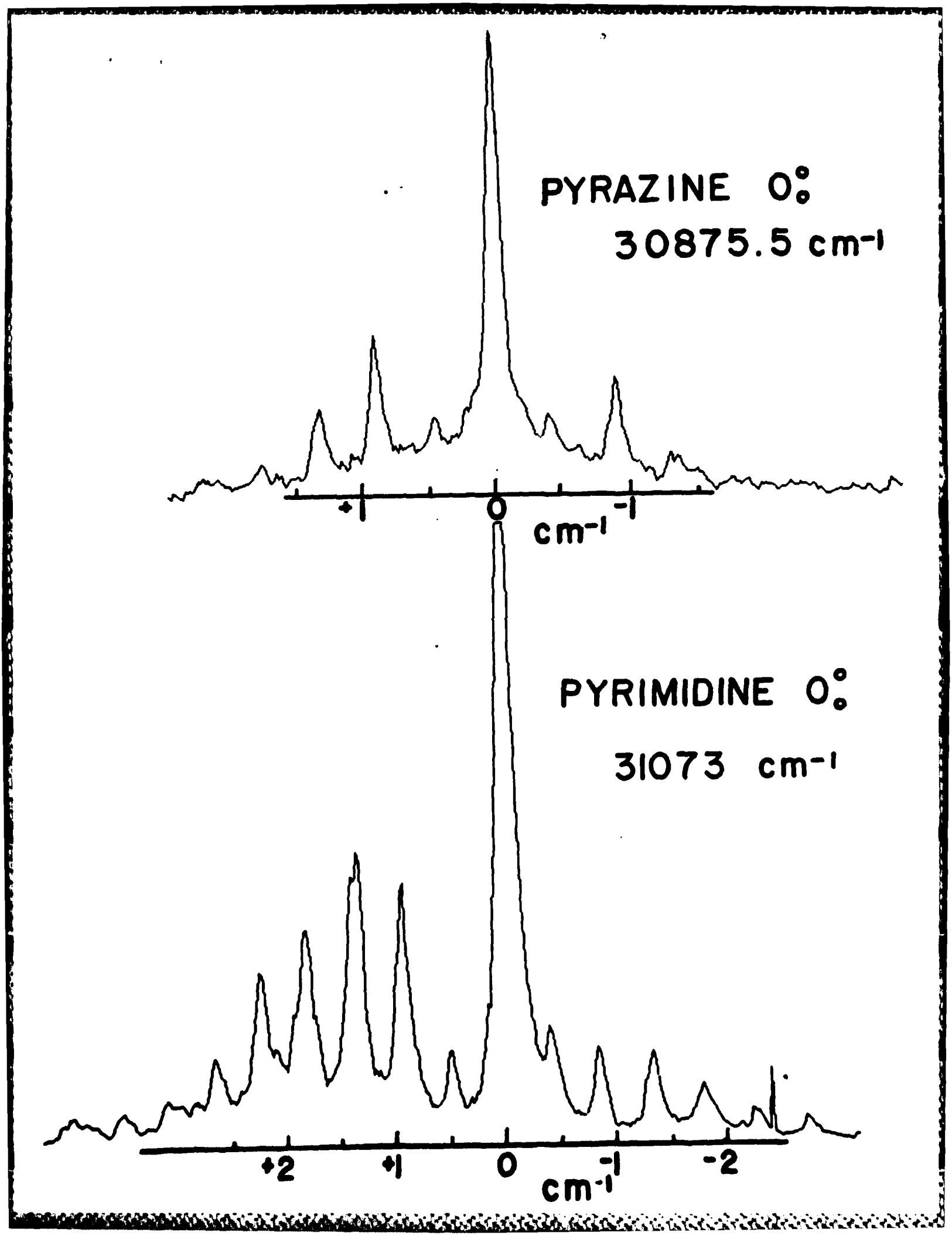
PYRAZINE 0°
30875.5 cm-1
+1
0
-1
cm-1
PYRIMIDINE 0°
31073 cm-1
+2
+1
0
-1
-2
cm-1

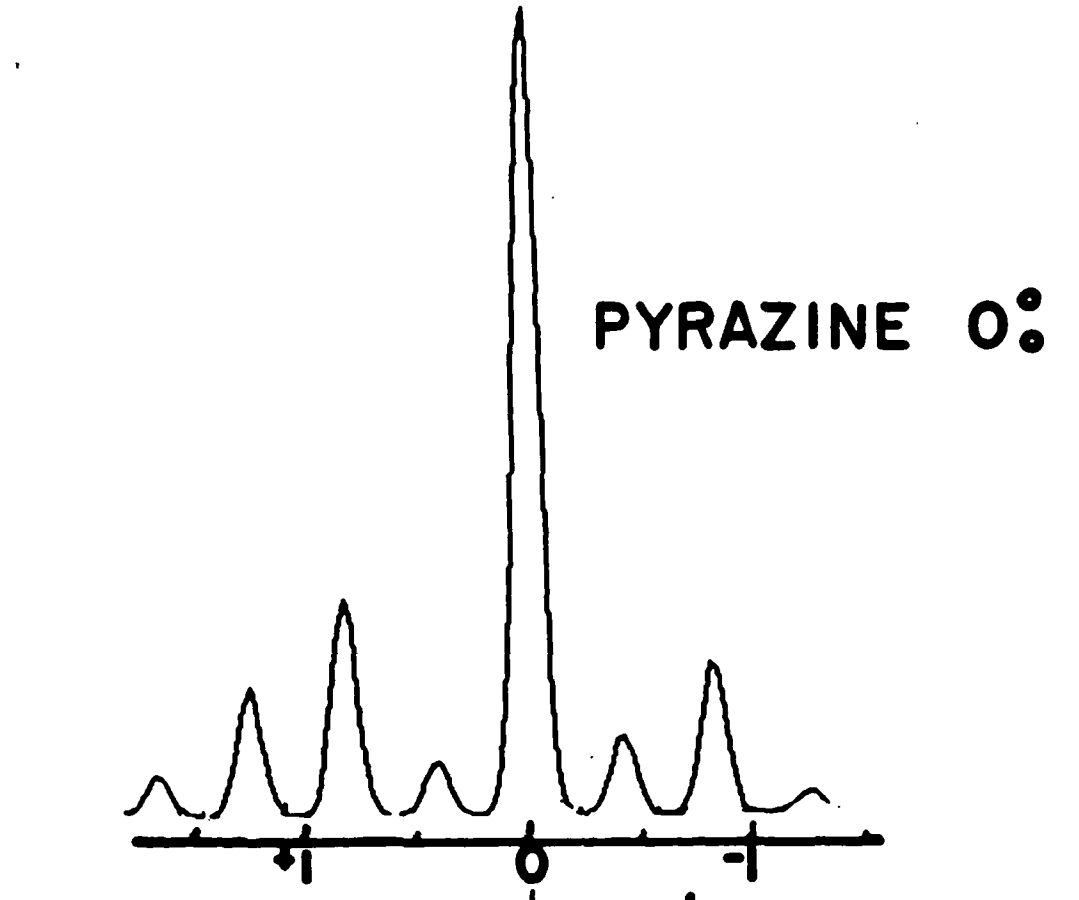
PYRAZINE 0°
+1
0
-1
cm⁻¹

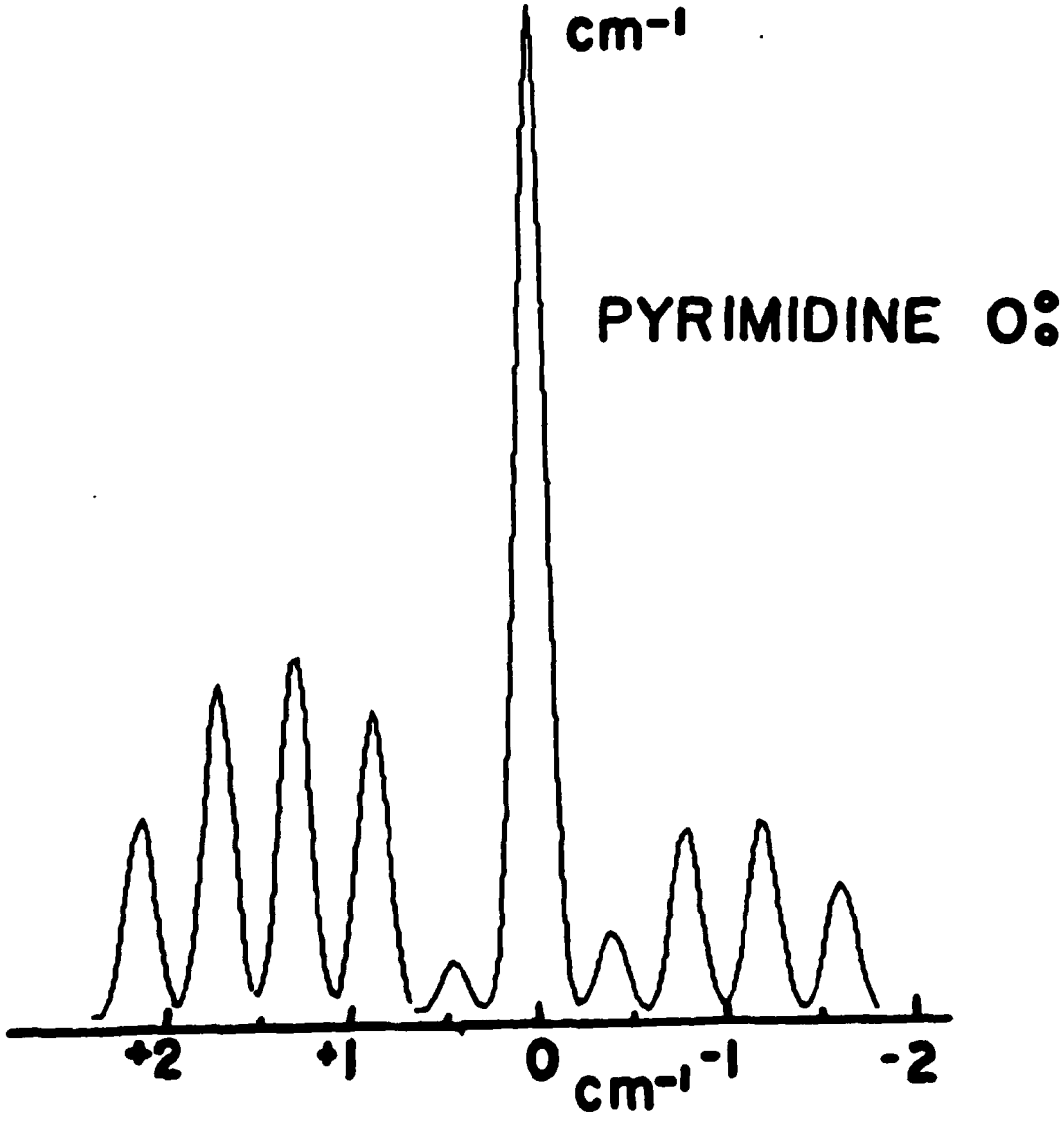
PYRIMIDINE 0°
+2
+1
0
cm⁻¹
-1
-2

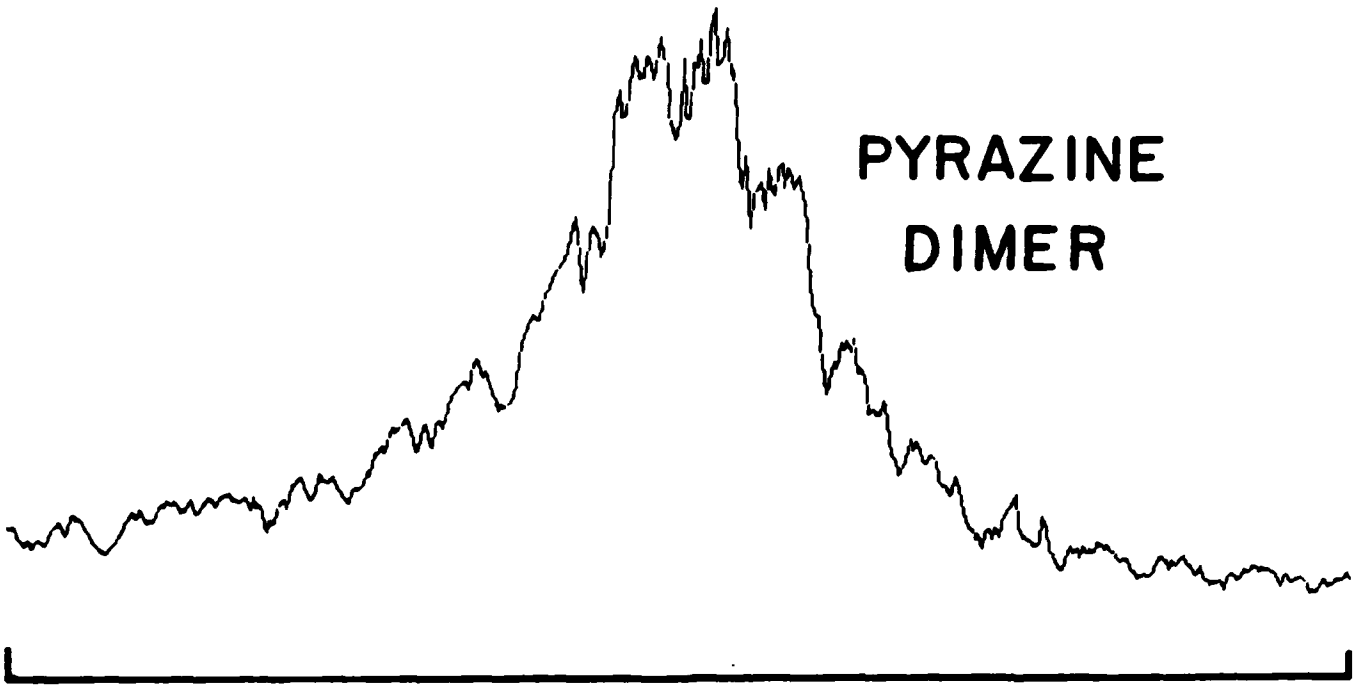

7.1 cm^{-1}

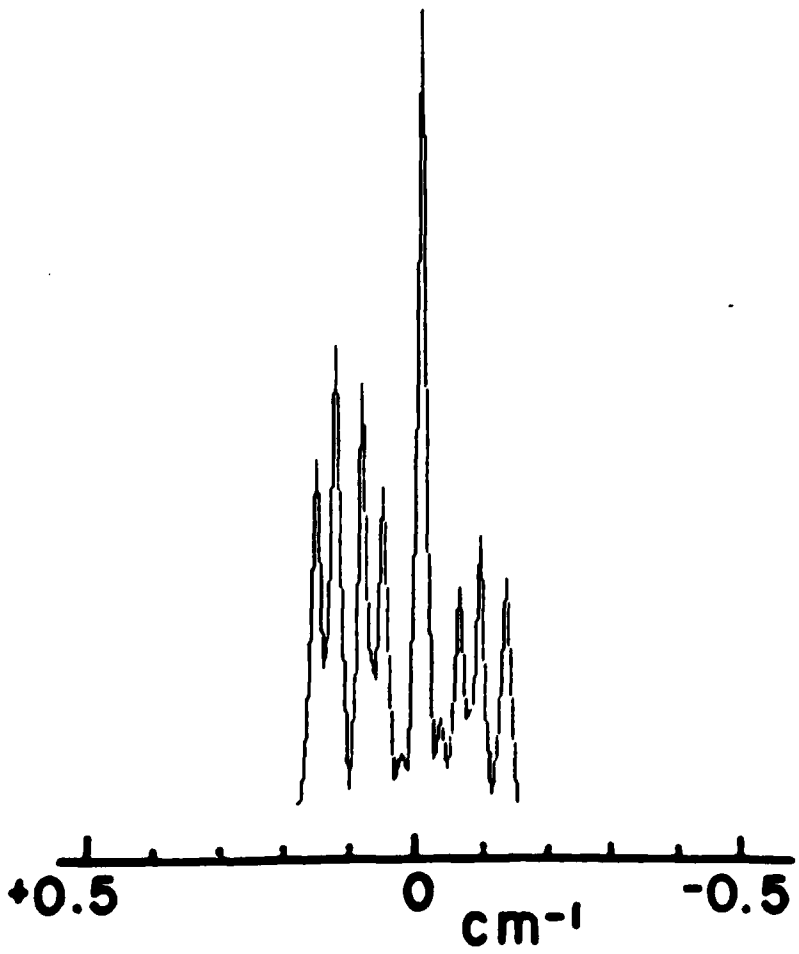

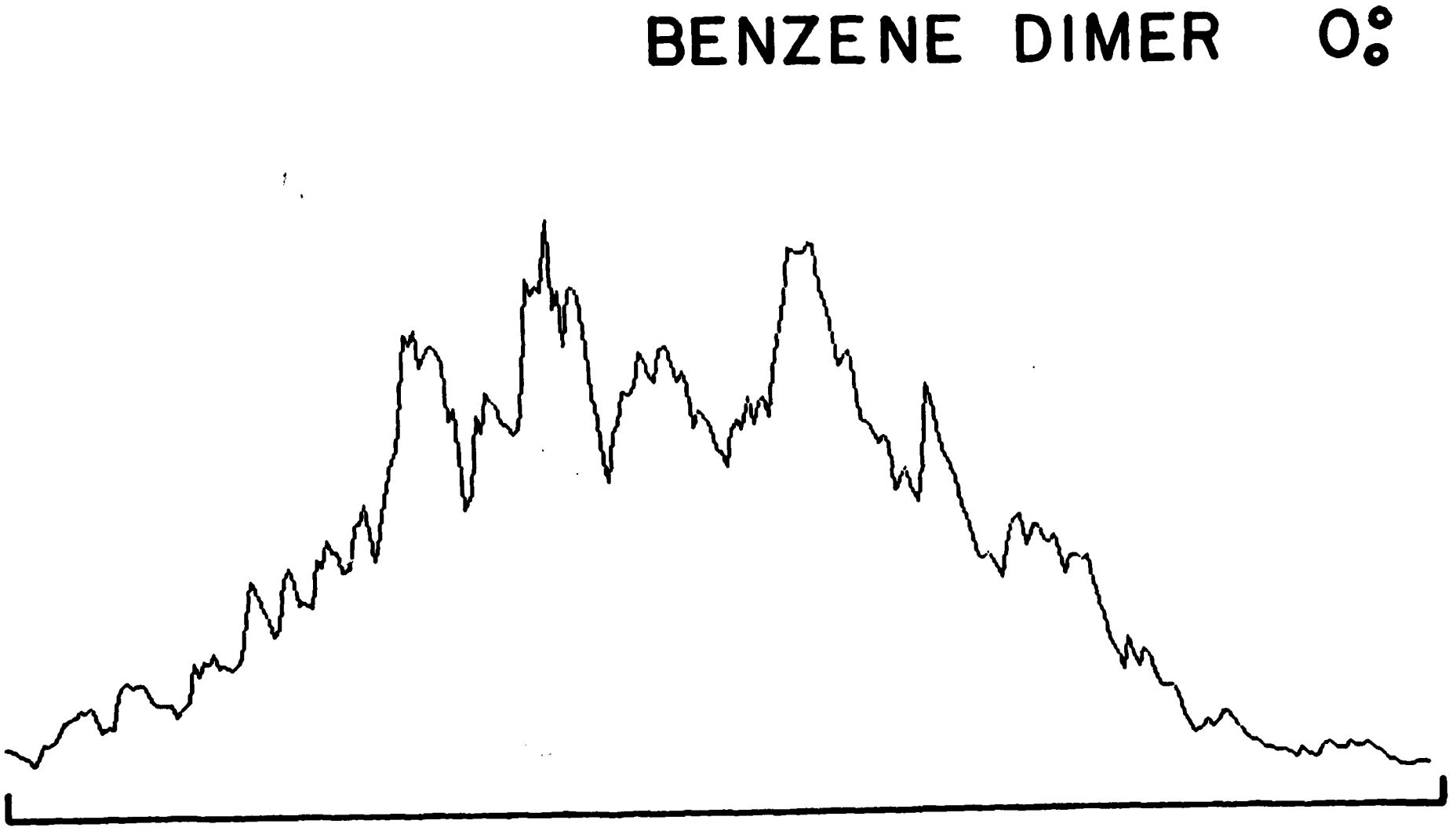
BENZENE DIMER 0°
5.9 cm⁻¹

s-TETRAZINE DIMER

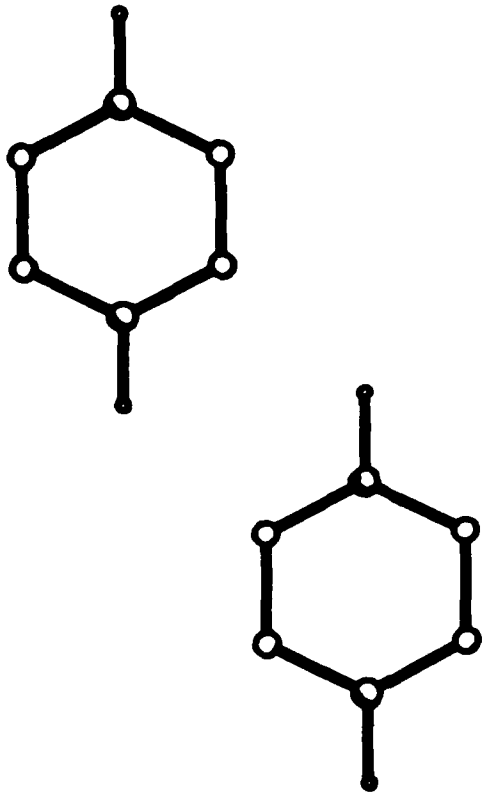

-658 cm^{-1}

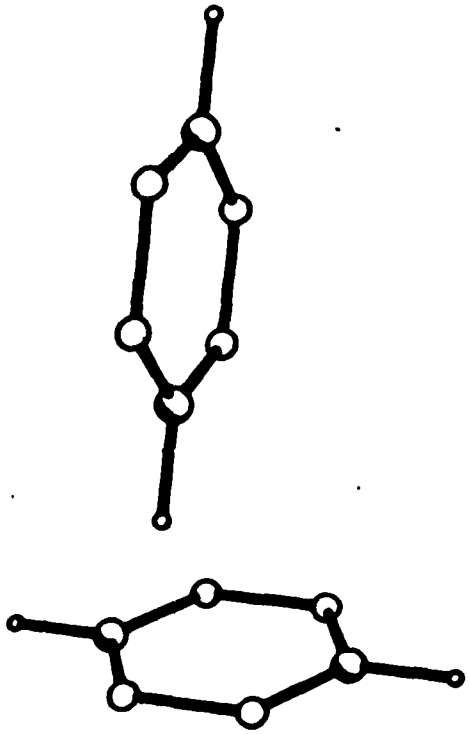

-955 cm^{-1}

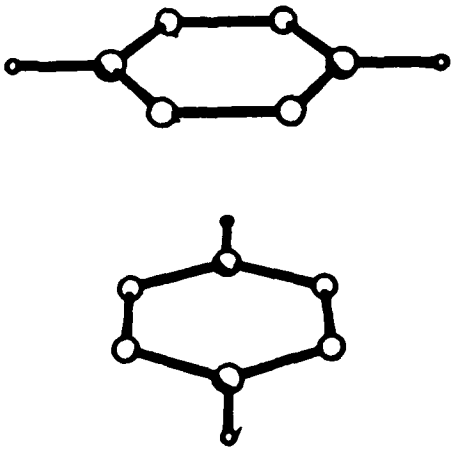

-1331 cm^{-1}

TETRAZINE DIMER

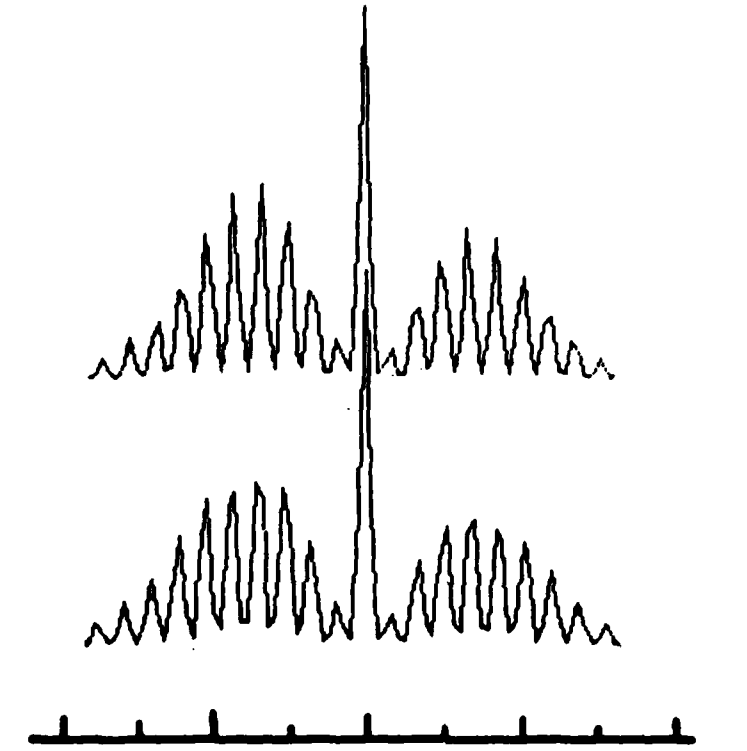

DL/413/83/01
GEN/413-2

TECHNICAL REPORT DISTRIBUTION LIST, GEN

	No. Copies
Office of Naval Research Attn: Code 413 800 N. Quincy Street Arlington, Virginia 22217	2
Dr. Bernard Douda Naval Weapons Support Center Code 5042 Crane, Indiana 47522	1
Commander, Naval Air Systems Command Attn: Code 310C (H. Rosenwasser) Washington, D.C. 20360	1
Naval Civil Engineering Laboratory Attn: Dr. R. W. Drisko Port Hueneme, California 93401	1
Defense Technical Information Center Building 5, Cameron Station Alexandria, Virginia 22314	12
DTNSRDC Attn: Dr. G. Bosmajian Applied Chemistry Division Annapolis, Maryland 21401	1
Dr. William Tolles Superintendent Chemistry Division, Code 6100 Naval Research Laboratory Washington, D.C. 20375	1
Dr. David Young Code 334 NORDA NSTL, Mississippi 39529	1
Naval Weapons Center Attn: Dr. A. B. Amster Chemistry Division China Lake, California 93555	1
Scientific Advisor Commandant of the Marine Corps Code RD-1 Washington, D.C. 20380	1
U.S. Army Research Office Attn: CRD-AA-IP P.O. Box 12211 Research Triangle Park, NC 27709	1
Mr. John Boyle Materials Branch Naval Ship Engineering Center Philadelphia, Pennsylvania 19112	1
Naval Ocean Systems Center Attn: Dr. S. Yamamoto Marine Sciences Division San Diego, California 91232	1

DL/413/83/01
051A/413-2

ABSTRACTS DISTRIBUTION LIST, 051A

Dr. M. A. El-Sayed
Department of Chemistry
University of California
Los Angeles, California 90024

Dr. E. R. Bernstein
Department of Chemistry
Colorado State University
Fort Collins, Colorado 80521

Dr. J. R. MacDonald
Chemistry Division
Naval Research Laboratory
Code 6110
Washington, D.C. 20375

Dr. G. B. Schuster
Chemistry Department
University of Illinois
Urbana, Illinois 61801

Dr. W. M. Jackson
Department of Chemistry
Howard University
Washington, D.C. 20059

Dr. M. S. Wrighton
Department of Chemistry
Massachusetts Institute of Technology
Cambridge, Massachusetts 02139

Dr. A. Paul Schaap
Department of Chemistry
Wayne State University
Detroit, Michigan 49207

Dr. Gary Bjorklund
IBM
5600 Cottle Road
San Jose, California 95143

Dr. G. A. Crosby
Chemistry Department
Washington State University
Pullman, Washington 99164

Dr. W. E. Moerner
I.B.M. Corporation
5600 Cottle Road
San Jose, California 95193

Dr. Theodore Pavlopoulos
NOSC
Code 5132
San Diego, California 91232

Dr. D. M. Burland
IBM
San Jose Research Center
5600 Cottle Road
San Jose, California 95143

Dr. John Cooper
Code 6170
Naval Research Laboratory
Washington, D.C. 20375

Dr. George E. Walrafen
Department of Chemistry
Howard University
Washington, D.C. 20059

Dr. Joe Brandelik
AFWAL/AADO-1
Wright Patterson AFB
Fairborn, Ohio 45433

Dr. Carmen Ortiz
Consejo Superior de
Investigaciones Cientificas
Serrano 117
Madrid 6, SPAIN

Dr. John J. Wright
Physics Department
University of New Hampshire
Durham, New Hampshire 03824

Dr. Kent R. Wilson
Chemistry Department
University of California
La Jolla, California 92093

END

11-86

DTIC